Mesua ferrea L. Seed Oil Based Highly Branched Polyester/Epoxy Blends and Their Nanocomposites

Uday Konwar, Gautam Das, Niranjan Karak

Advanced Polymer and Nanomaterial Laboratory, Department of Chemical Sciences Tezpur University, Napaam 784028, Tezpur, Assam, India

Received 26 May 2010; accepted 13 November 2010
DOI 10.1002/app.33743
Published online 25 February 2011 in Wiley Online Library (wileyonlinelibrary.com).

ABSTRACT: *Mesua ferrea* L. seed oil based highly branched polyester and epoxy resins blends were prepared by mechanical mixing at different weight ratios. The best performing blend was used as the matrix for the preparation of nanocomposites with different dose levels of organophilic montmorillonite (OMMT) nanoclay. The prepared nanocomposites were characterized by X-ray diffraction, scanning electron microscopy, Fourier transform infrared spectroscopy, and transmission electron microscopy. Data resulting from the mechanical and thermal studies of the blends and nanocomposites indicated improvements in the tensile strength and thermal stability to appreciable extents for the nanocomposites with OMMT loading. The nanocomposites were characterized as well-dispersed, partially exfoliated structures with good interfacial interactions. From the X-ray diffraction analysis, the absence of d_{001} reflections of the OMMT clay in the cured nanocomposites indicated the development of an exfoliated clay structure, which was confirmed by transmission electron microscopy. The homogeneous morphologies of the pure polyester/epoxy blend and clay hybrid systems were ascertained with scanning electron microscopy. The tensile strength of the 5 wt % clay-filled blend nanocomposite system was increased by 2.4 times compared to that of the pure blend resin system. The results suggest that the prepared nanocomposites have the potential to be used as active thin films for different applications. © 2011 Wiley Periodicals, Inc. J Appl Polym Sci 121: 1076–1085, 2011

Key words: nanocomposites; polyesters; polymer blends; renewable resources; resins

INTRODUCTION

In recent days, the significance of natural assets for industrial applications has become exceedingly apparent with increasing emphasis on environmental issues, waste disposal, and depletion of nonrenewable resources.[1] Polymers from renewable resources can form a basis for the replacement or substitution of petroleum-based polymers through the inventive design of new biobased polymers that can contend with or even surpass existing petroleum-based materials from the social, environmental, and cost viewpoints.[2]

Vegetable-oil-based polyester resins have a wide range of industrial relevance, such as in industrial finishes and maintenance, architectural uses, paints, and surface coatings.[3] These resins have a number of advantages, including versatility in structure and properties, overall low cost, and ease of application.[4] However, they suffer from some decisive drawbacks, such as low mechanical properties, alkali resistance, and low hardness.[5] So, to improve these drawbacks of polyester resins, blending with other suitable resins, such as epoxy resin, amino resin, silicone resin, and ketonic resin, can be performed, as polyester resins have good compatibility with a wide variety of other resins.[6] The better compatibility comes from the relatively low viscosity of the resin and from the structure of the resin, which contains a relatively polar and aromatic backbone and aliphatic side chains with low polarity.[7] The blending technique may be used effectively to improve the inferior properties of both the components. Miscible polymer blends produce a new improved material from less superior individual components, but well-established miscible polymer blends are very rare to obtain.[8,9] However, semimiscible blends with a uniform distribution of components also improve properties to an acceptable range.[10] Again, because of their compact three-dimensional structure with a high surface functionality and lack of restrictive interchain entanglements, highly branched polymers show a lower melting point and solution viscosity than their linear analogs.[11] Also, because of their high density of tailorable end groups on the surface, they can effectively function as blend components with other polymers.

Correspondence to: N. Karak (karakniranjan@yahoo.com).
Contract grant sponsor: Defense Research and Development Organization (India); contract grant number: ERIP/ER/0403490/M/01/962.

Epoxies obtained from vegetable oils are marked by good adhesion, flexibility, and corrosion-resistance properties.[12] These attributes of oil-based epoxies render them suitable for versatile applications as plasticizers, diluents, and corrosion-protective coatings. Thermoset epoxy resins are widely used in coatings, adhesives, molding compounds, and polymer composites because of their superior thermomechanical properties and excellent processability.[13] However, the use of thermosetting materials is often limited because of a toughness problem. Therefore, the bulk amounts of epoxies, when used, are usually blended with tougheners, mostly rubber particles, and used as the second phase in the resin system. However, these particles always affect the processability of the system. Because of the flexibility present in the structure of a vegetable-oil-based epoxy, it could be used as one blend component in this study. It also has large numbers of epoxy and hydroxyl groups, which may take part in crosslinking reactions with oil-modified polyester resins. In addition to blends of natural polymers,[14] so far, no report has been published on the utilization of vegetable-oil-based resins as the sole blend components. Because of the presence of long-chain fatty acids in vegetable oil, the used blend components have advantages, such as an ease of processability and compatibility. Again, because of the enhancement of the properties, such as the mechanical, thermal, and barrier properties, even at low concentrations, the nanocomposites of such blends have drawn much attention.

Nanocomposites from natural resources have attracted significant interest because these materials have social, environmental, and economic advantages. Polymers reinforced with nanoclays have been shown to exhibit enhancements in mechanical, thermal, and barrier properties at a low concentration of clay.[15,16] The importance of inorganic–organic hybrids as an alternative to conventional coatings as cost-effective and high-performance coatings is due to their unusual, tailor-made material properties, which arise from the distinctive combination of the properties of the inorganic and organic counterparts. The attractive improvement results from the synergistic effect between the organic and inorganic components and the large interfacial coupling.

Among different polymers[17–21] made from *Mesua ferrea* L. seed oil, highly branched polyester and epoxy resins have already been proven their potential as surface-coating materials. So, in this study, these resins were used as vegetable-oil-based blend components. Therefore, we report here the study of *M. ferrea* L. seed oil based highly branched polyester/epoxy resins blends at different weight ratios and their performances. Using the best-studied blend system as a matrix, we also investigated the preparation, characterization, and properties of the nanocomposites with organophilic montmorillonite (OMMT).

EXPERIMENTAL

Materials

M. ferrea L. seed oil was isolated from nahar seeds (Sivasagar, Assam). 52.3% Oleic acid and 22.3% linoleic acid as unsaturated fatty acids and 15.9% palmitic acid and 9.5% stearic acid as saturated fatty acids were present in the pure oil.[22] Phthalic anhydride, maleic anhydride, 2,2-bis(hydroxymethyl) propionic acid, glycerol (Merck, Hohenbrunn, Germany), and lead monoxide (S.D. Fine Chemical, Ltd., Merck, Mumbai, India) were used without further purification. OMMT (Nanomer I.30E, montmorillonite clay modified with 25–30 wt % octadecylamine, Sigma–Aldrich, Taufkirchen, Germany) was used as nanofillers for the system. *N,N*-Dimethylformamide (Merck, Mumbai, India) and xylene (Merck, Mumbai, India) were used as solvents after distillation. Epichlorohydrin (Merck, Mumbai, India) and bis(4-hydroxyphenyl) sulfone [bisphenol S (BPS); Sigma–Aldrich, Taufkirchen, Germany] were used as received. Polyester resin (acid value = 10.66 mg of KOH/g, saponification value = 280.5 mg of KOH/g, viscosity = 48.01 Pas) of *M. ferrea* L. seed oil was obtained by a method reported earlier.[21] Bisphenol A (BPA; BG and Co., Mumbai, India) was used after purification by recrystallization from toluene. *M. ferrea* L. seed oil based sulfone-containing epoxy resin[23] (epoxy equivalent = 447 g/equiv, hydroxyl value = 250 mg of KOH/g), synthesized from the monoglyceride of *M. ferrea* L. seed oil, BPS, BPA, and epichlorohydrin, was used as a one of the blend components. Poly(amido amine) hardener (HY 840, Ciba Geigy, Mumbai, India), with an amine value 6.6–7.5 equiv/kg, was used as supplied. All other reagents were reagent grade and were used without further purification.

Methods and instrumentation

After collection through a solvent-soaking method from matured Nahar seeds, the *M. ferrea* L. seed oil was purified by an alkali-refining technique.[22] *M. ferrea* L. seed oil based polyester resin[21] and epoxy resin[23] were prepared as reported earlier. An ultrasonicator (UP200S, Hielscher, Teltow, Germany) was used at a fixed amplitude and in a continuous cycle for dispersion of the OMMT. The Fourier transform infrared (FTIR) spectra of the pristine blend and the nanocomposites were obtained with a Nicolet FTIR Impact 410 spectroscope (Madison, WI) with KBr pellets. X-ray diffraction (XRD) was carried out at a scanning rate of 0.05°/min over the range 2θ = 0–30° with a Rigaku X-ray diffractometer (Miniflex, Tokyo, Japan). Thermogravimetric analysis (TGA) of

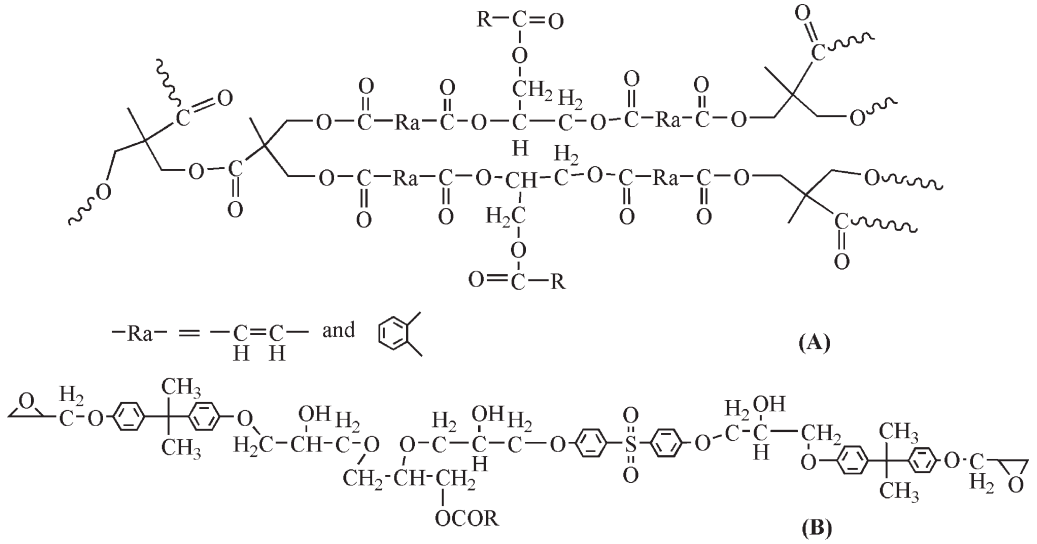

Figure 1 Representative chemical structures of (A) the highly branched polyester and (B) the epoxy resin based on *M. ferrea* L. seed oil.

the cured nanocomposites was carried out with a Shimadzu thermal analyzer (TGA 50, Tokyo, Japan) under a nitrogen flow rate of 30 mL/min and a heating rate of 10°C/min. The polyester/epoxy blends and nanocomposites were applied on commercially available standard-size mild steel strips (150 × 50 × 1.60 mm^3) and glass plates (75 × 25 × 1.75 mm^3) for the determination of gloss by a digital mini gloss meter (Sheen Instrument, Ltd., Surrey, United Kingdom) at 60°, scratch hardness by a scratch hardness tester (Sheen Instrument, Ltd., Surrey, United Kingdom), impact resistance by a falling weight impact tester (SC Dey, Kolkata, India), and chemical resistance[18] by the ASTM D 593-67 (in brine, water, acid, and alkali) performance of coated panels. The surface morphology of the nanocomposites films was observed with a JSM-6390LV scanning electron microscope (JEOL, Tokyo, Japan) after they were coated on platinum through carbon strips. The size and distribution of the OMMT layers in the nanocomposites were studied with a JEOL JEMCXII transmission electron microscope at an operating voltage of 20–100 kV. For the determination of the tensile strength, the cured nanocomposites films were cut to a uniform thickness of 0.8–1 mm, a width of 10 mm, and a length of 7–8 cm. The tensile strength of the nanocomposite films was measured with a Z010 universal testing machine (Zwick, Ulm, Germany) with a 10-kN load cell and at jaw separation speed of 50 mm/min under ambient conditions. Swelling (percentage) was measured by differences in the weights between the dried film and the swollen film of the nanocomposites. Xylene was used as the solvent to swell the films. The weight of the swollen film was measured after 48 h until a constant weight was obtained. Before we measured the weight, the swollen films were blotted quickly between sheets of blotting paper after they were taken out of the solvent. The swelling percentage was calculated as follows:

$$\text{Swelling}\,(\%) = [(W_s - W_d)/W_d] \times 100$$

where W_s and W_d are the weights of the swollen and dried films, respectively.

Preparation of the polyester resin

The polyester resin was prepared as reported earlier.[21] Briefly, 0.12 mol (42.09 g) of monoglyceride, 0.064 mol (6.27 g) of maleic anhydride, and 0.096 mol (14.22 g) of phthalic anhydride were reacted together to form the carboxyl terminated prepolymer. An amount of 20 g of this prepolymer was then reacted with 3.32 g (0.016 mol) of 2,2-bis(hydroxymethyl) propionic acid to obtain the desired resin. The representative chemical structure of the resin is shown in Figure 1.

Preparation of the epoxy resin

The vegetable-oil-based epoxy resin was prepared as described in our earlier article.[23] We treated monoglyceride of the oil (obtained by the glycerolysis technique), epichlorohydrin, BPA, and BPS together by maintaining a molar ratio of 1 : 8 : 2 : 1 at 110 ± 5°C for 8 h in a slightly alkaline medium. After the completion of the reaction, the product was separated in a separating funnel and washed with a brine solution and distilled water. Then, the product was vacuum-dried to obtain the product at a 80–90%

TABLE I
Compositions of the Blends and Nanocomposites

Sample code	Polyester resin (g)	Epoxy resin (g)	Hardener (g)	Clay loading (g)
PEB1	30	70	35	0
PEB2	40	60	30	0
PEB3	50	50	25	0
PEB4	60	40	20	0
BNC1	30	70	35	1
BNC2.5	30	70	35	2.5
BNC5	30	70	35	5

yield. The representative chemical structure of the resin is shown in Figure 1.

Preparation of the blends and nanocomposites and their curing

M. ferrea L. seed oil based highly branched polyester and epoxy resins were placed in a vacuum oven at 50°C before the preparation of blends to remove trapped air, moisture, and volatiles. The polyester and epoxy resins were mixed at predetermined ratios of 30/70, 40/60, 50/50, and 60/40 (w/w) to obtain the PEB1, PEB2, PEB3, and PEB4 blends, respectively, along with the required amount of poly(amido amine) hardener (Table I). We added the hardener in each case and maintained the ratio of epoxy to hardener at 2 : 1 (w/w). Each of these samples was mixed under continuous agitation by mechanical stirring for 30 min. The blends were left at ambient temperature for 24 h under observation. No visual phase separation was observed; this indicated proper mixing with good interaction between the two constituents.

Different dose levels (Table I) of OMMT were dispersed in xylene by mechanical shearing for 30 min; this was followed by ultrasonication for 10 min. Separately, we mechanically mixed the polyester resin and epoxy resin at a 30 : 70 weight ratio (PEB1) by stirring for 30 min. The dispersed clay was then mixed with the previous mixture under vigorous mechanical stirring followed by ultrasonication for 30 min. After sonication, a 50% poly(amido amine) hardener (with respect to epoxy resin) was added into the mixture and degassed for about 20 min *in vacuo* until it was completely bubble free. Then, the mixture was cast onto mild steel plates (150 × 50 × 1.60 mm^3) and glass plates (75 × 25 × 1.75 mm^3) and dried *in vacuo* in a desiccator for overnight at room temperature. Then, it was allowed to cure at 120°C for further study.

The curing time was estimated on the basis of the hard drying time of the cast thin films of the blends or the nanocomposites on glass plates. The hard drying time was determined as the minimum time required to cure the film (40–50 μm thickness as measured by the Pen tester, Sheen Instrument) at the specified temperature by the measurement of the resistance to indentation by an indenter (pin).

RESULTS AND DISCUSSION

Formation of the polyester/epoxy blends and nanocomposites

The blends of polyester and epoxy resins were prepared at different compositions (Table I) under mechanical agitation in the absence of any solvent. As there was no visible phase separation between the polyester and epoxy resins in the prepared blends, even after sufficient storage time, we concluded that the components were completely miscible with each other and the hardener. This was attributed to the strong intermolecular interactions in the form of hydrogen bonding and polar–polar interactions between the components through the ester, epoxide, and other groups. Such good miscibility between the components eventually had positive effects on the entanglements of the chains and network structures.

Polymers have frequently been used as matrixes in the preparation of nanocomposites because they prevent the agglomeration and settling of the nanoparticles. The addition of clay to triglyceride-based polymeric blends to form nanocomposites can broaden the applications of these new biobased materials by improving their mechanical properties.[24–27] Among the vast nanoreinforcements available for the fabrication of polymer nanocomposites, researchers have focused on and studied clays the most because they are naturally occurring minerals, exhibit a layered morphology with high aspect ratios, and have substantial cation-exchange capacities. In this study, OMMT was used as a nanofiller for the proper dispersion of the clay layers with the matrix. To make the polymer chain molecules penetrate into the OMMT basal interspacing, a strong mechanical force is commonly applied to a dry blend of clay and melted polymer. In this study, mechanical agitation with a high shear force and ultrasonication was only applied to the mixture of the clay and polyester–epoxy blended matrix to obtain delaminated clay layers. The carboxyl groups of the polyester resin and epoxy groups and hydroxyl groups of the epoxy resin easily interacted with the hydroxyl groups of the nanoclay through hydrogen bonding or other polar–polar interactions to form stable and well-dispersed nanocomposites.

Characterization of the blends and nanocomposites

XRD analysis

Figure 2 shows the XRD patterns for the pristine polyester/epoxy blend and its nanocomposites with

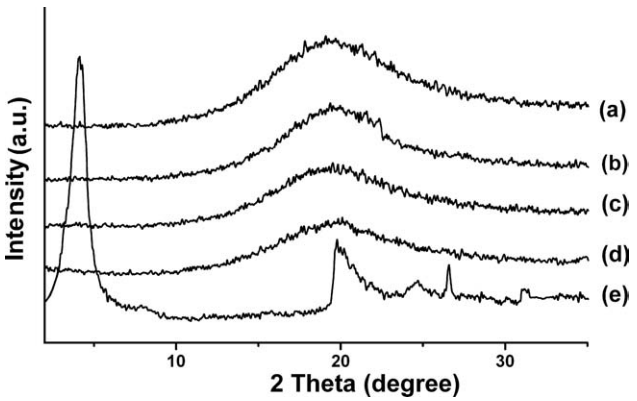

Figure 2 XRD traces for (a) PEB1, (b) BNC1, (c) BNC2.5, (d) BNC5, and (e) OMMT.

different clay contents. Organically modified MMT showed a basal reflection peak (d_{001}) at an angle of 4.17° (2θ), which corresponded to a *d*-spacing of 2.36 nm. The characteristic diffraction peak of the clay disappeared in the XRD pattern of the blend nanocomposite with 0–5 wt % OMMT in the angular range of the study. The absence of the peak probably suggests the delamination and dispersion of the clay nanolayers within the polyester–epoxy blend matrix, that is, the formation of an exfoliated structure. This was due to the compatibility of polyester and epoxy resins with the layered silicates, and the polymer chain penetrated into the clay galleries and expanded them. In the pristine blend, a broad peak at 20° was observed and appeared to be due to the amorphous nature of the polyester and the epoxy resin. Although it is a common practice to define a nanocomposite as an exfoliated one by the absence of a peak at [001] reflection, nevertheless, it is difficult to reach a final conclusion about the actual structure from XRD alone. The dispersion of the OMMT in the polyester–epoxy blend matrix was attributed to its improved thermomechanical characteristics.

Scanning electron microscopy (SEM) analysis

To determine the OMMT dispersion in the polyester–epoxy blend matrix, we observed the surface morphology of the blend nanocomposite films from SEM images (Fig. 3). As shown in Figure 3, a smooth surface was observed in the blend matrix; this supported the miscibility without any phase separation of the two blend components, whereas a uniform distribution of clay layers or lines with a smooth surface was observed in the nanocomposites. This indicated that the clay layers were well dispersed and embedded in the matrix. With the increase of clay loadings, the well-dispersed layers or lines also increased in the matrix.

Transmission electron microscopy (TEM) analysis

The morphology and the actual structure or pattern of the clay layer dispersion in the polyester/epoxy blend was further analyzed by TEM. It has been reported in the literature that increasing clay loading enhances the ordering of clay platelets and gradually enervates the exfoliation potential of the polymer. This is ascribed to the increased viscosity, which

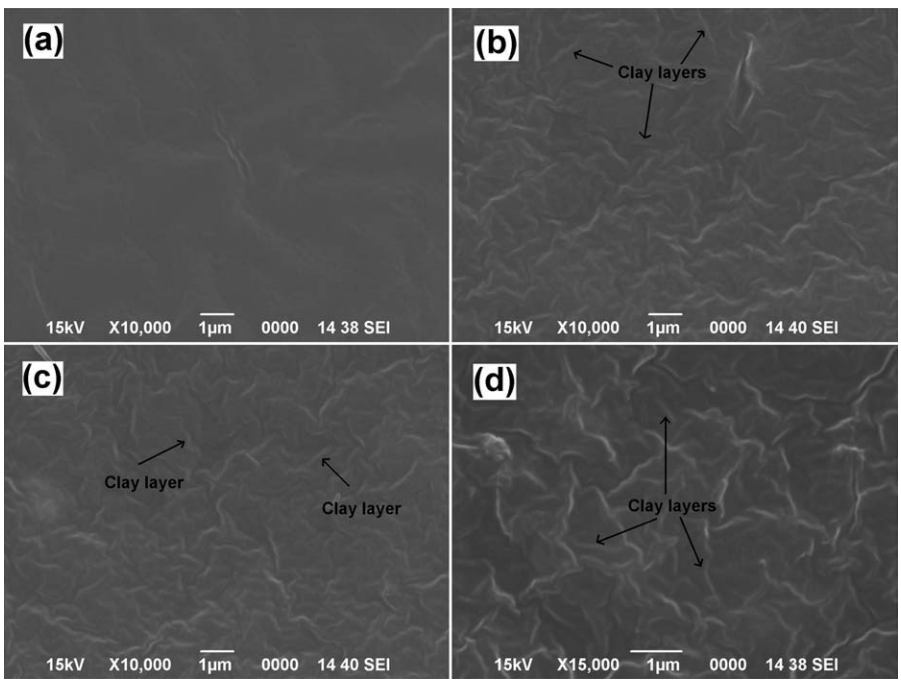

Figure 3 SEM micrograms for (a) PEB1, (b) BNC1, (c) BNC2.5, and (d) BNC5.

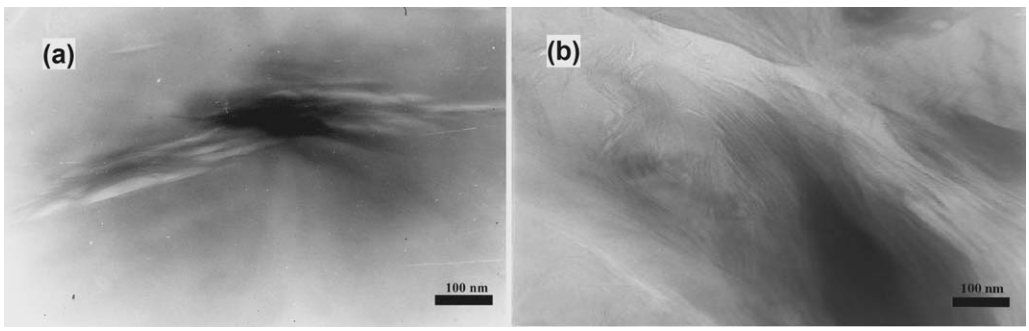

Figure 4 TEM micrograms for (a) BNC2.5 and (b) BNC5.

impedes the ease of the melt flow and causes the stabilization of the flow; this hinders the complex flow patterns and agitation necessary to break apart the tactoids. Moreover, in high loadings of organoclay, silicate–silicate interactions, which impede the dispersion of the layers, become more probable. A homogeneous dispersion of clay platelets, with an average thickness in the range 25–30 nm, was observed in the TEM images (Fig. 4) of the nanocomposites. Upon nanocomposite formation, the individual clay layers were found to be disintegrated or partially exfoliated and well dispersed in the polymer matrix. Also, the individual clay layers and zones with more than one clay layer were noted in the TEM images. The reason for this excellent distribution was the strong interactions between the polar carboxylic ester groups of the polymer and the —OH group of clay and hydrophilic character of both components.

FTIR analysis

In the FTIR spectra (Fig. 5) of the cured blend, we observed the shifting of C=O band of ester in the *M. ferrea* L. seed oil based polyester resin (spectrum not shown)[28] from 1736 to 1743 cm^{-1}. This was due to the interaction of the polyester resin with the epoxy resin and the hardener. The band for the epoxide group at 914 cm^{-1}, which was present in epoxy resin (spectrum not shown) with a significant intensity, decreased in intensity in the blend; this indicated a reaction between the epoxy and the curing agent.[29]

In the nanocomposites, the carbonyl stretching frequency was observed to shift toward a lower value (1720–1731 cm^{-1}) than that of the blend. This shifting was attributed to the interaction of polyester segments (—COOH and —OH) with the —OH group of OMMT through hydrogen bonding or other polar–polar interactions.[18] The bands due to Si—O—Si (1030 cm^{-1}) and Al—O—Al (550 cm^{-1}) stretching vibrations of OMMT were observed to broaden in the nanocomposites with 0–5 wt % OMMT loading. Also, the band at 3465 cm^{-1} due to the —OH stretching vibration frequency of the polyester resin was shifted toward a lower wave-number region (3443 cm^{-1}) after nanocomposite formation because of the overlap with the —OH group of OMMT. These results show strong interactions between the different components present in the nanocomposite system. The interaction of the ester/—OH group of the polymer chains or the amino group of the hardener with the —OH group of OMMT could be put forward for the same.

Curing study of the blends and nanocomposites

There was a possibility of crosslinking by the hydroxyl groups of the polyester resins originally present in the fatty acid or generated during the crosslinking reactions with the epoxy groups of the epoxy resin in the presence of the amine hardener, which was an active base. Furthermore, hydrogen bonding between C=O of the polyester resins with —OH of the epoxy resin present in the system occurred. Also, there was a possibility of chemical reactions of the hydroxyls/epoxides of the epoxy resin with the hydroxyl groups of the polyester resin in the presence of the amine hardener along with reactions of the hydroxyl/ester groups of the polyester resin with amine groups of the hardener.

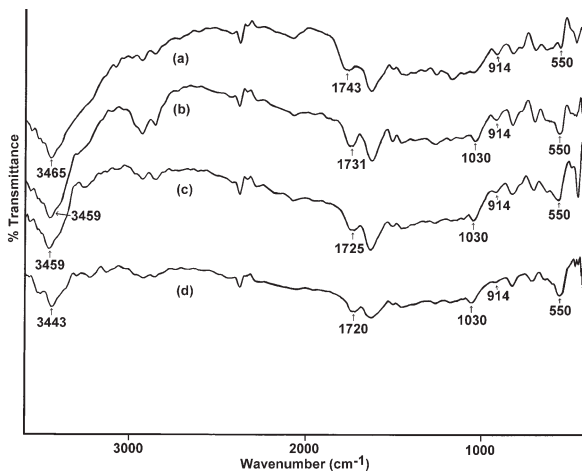

Figure 5 FTIR spectra for (a) PEB1, (b) BNC1, (c) BNC2.5, and (d) BNC5.

TABLE II
Performance Characteristics of the Blends and Nanocomposites

Property	PEB1	PEB2	PEB3	PEB4	BNC1	BNC2.5	BNC5
Gloss at 60°	82	90	102	110	90	95	103
Scratch hardness (kg)	5	4.4	4	3	5.5	7	8
Impact resistance (cm)	65	50	45	45	75	80	84
Tensile strength (N/mm^2)	2.7	2.04	1.96	1.78	3.26	4.92	6.42
Elongation at break (%)	52	41	30	24	79	104	137
Curing time at 120°C (min)	80	120	180	300	75	60	50
Swelling in xylene (%)	28.5	30	33.4	36.2	25	24.35	22

Furthermore, the hydroxyl groups of the epoxy resin may have undergone a self-condensation reaction to form ether linkages. This explained the high rate of curing of the epoxy resin by the amine hardener and the blend system.

In the nanocomposites, the curing rate increased with increasing clay loading compared to the blend (Table II). This increase was ascribed to the restricted mobility of the polymer segments. Because of the high surface area of OMMT, it interacted with the polymer chains and restricted the mobility of the molecular chains and took part in a crosslinking reaction via interaction through the hydrogen bonding between the —OH group of OMMT/polyester and with the —OH of the epoxy resin and —NH of the amine hardener.

Performance characteristics of the blends and nanocomposites

With a perfect distribution of the reinforcing OMMT in the matrix, the observed values for different performance characteristics, such as tensile strength, elongation at break, gloss, impact resistance, and scratch hardness, of the prepared blends and nanocomposites films are presented in Table II.

An improvement in the tensile strength of the polyester/epoxy blends was observed from PEB4 to PEB1. This was due to the increase in the epoxy content in the blend and the good crosslinking density in the cured blend structure, as supported by the swelling values (Table II). In the blend nanocomposites, the tensile strength increased to a noticeable degree from 2.7 to 6.42 N/mm^2 with increasing OMMT loading from 0 to 5 wt %. This increase in the tensile strength was attributed to the uniform distribution of OMMT and the good interfacial adhesion between the clay layers and the polymer matrix.[30] This well-dispersed OMMT with good interfacial interactions with the polyester matrix could have constrained the segmental motions of the polymer chains by delaminating the OMMT; this resulted in the strengthening of the polyester matrix. Also, after delamination of the aluminosilicate OMMT, the maximum surface of the silicate layers was available for strong interaction with the polymer chains; this led to an increase in the tensile strength. The addition of the vegetable-oil-based epoxy resin increased the flexibility of the blends, as observed experimentally as an enhanced elongation at break with clay loading. The addition of OMMT enhanced the blend flexibility and, hence, increased the ductility. The increase in the elongation at break with increased clay content was also caused by the presence of the long hydrocarbon chain of the fatty acid and the internal bond strength rather than the crosslink density. With increasing OMMT content, the increase in the elongation at break was mainly attributed in part to the plasticizing effect of the gallery oniums, which contributed to the formation of dangling chains. It may also have been due to conformational effects at the polyester matrix/clay interface and also to the enhanced stress-bearing capability of the nanocomposites.[31] Elongation is a property influenced more seriously by chain breakage than chain slippage.[32]

Gloss refers to specular reflection or the light reflected at the same angle as the angle of incidence. The gloss of the coated surface depends on the amount of light absorbed or transmitted by the coating material and is influenced by the smoothness or texture of the surface. In general, polyesters show good gloss, much higher than epoxy resin. Thus, the epoxy resin had low gloss characteristics, which were improved by the blending with polyester resins in all of the cases. This improvement may have been due to the improved compatibility of these blends and good light stability of the polyester resins, for which the blends showed good gloss. A smooth surface obtained because of the better crosslinking of the cured films led to the augmentation of the gloss characteristics of the films after nanocomposite formation. This escalation resulted because of the better compatibility of the blend components with the clay. The gloss value increased with increasing clay content, as a large amount of light was reflected from the smooth surface.

Scratch hardness arose from the resistance of the materials to the dynamical surface deformation, that is, ploughing, and from the interfacial friction between the indenter surface and the material.[33]

TABLE III
Chemical Resistance of the Blends and Nanocomposites

Code	Alkali (5%)	HCl (25%)	NaCl (25%)	Distilled water
PEB1	Good	Excellent	Excellent	Excellent
PEB2	Good	Excellent	Good	Good
PEB3	Peeled off	Good	Good	Good
PEB4	Peeled off	Good	Good	Good
BNC1	Excellent	Excellent	Excellent	Excellent
BNC2.5	Excellent	Excellent	Excellent	Excellent
BNC5	Excellent	Excellent	Excellent	Excellent

Scratch hardness represents the response of the material under serious dynamic surface deformation, which involves highly localized strain field and material failure in a plastic and/or brittle manner, depending on the nature of the scratched materials. The value of scratch hardness for the polyester–epoxy blend system increased with increasing amount of epoxy resin (Table II). This was due to the interaction of the hydroxyl groups of the highly branched polyester resin with the epoxide groups of the epoxy resin and also with the poly(amido amine) hardener. With increasing epoxy resin amount, the crosslinking density of the blend system increased with the crosslinked structure of the highly branched polyester and epoxy system. Again, a significant improvement was observed in the values of scratch hardness after nanocomposite formation when the blend system was reinforced with 0–5 wt % OMMT; this confirmed effective network formation. The adept restriction of indentation by the uniformly disseminated OMMT in the nanocomposites may have resulted in this enhancement in scratch hardness.

The impact resistance of the polyester–epoxy blends increased with epoxy content (Table II). This may have been due to the perfect interfacial bonding between the polyester and epoxy by the contribution

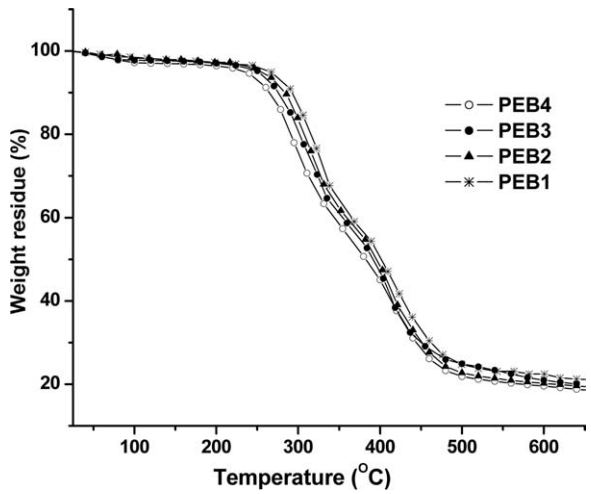

Figure 6 TGA thermograms for the polyester/epoxy blends.

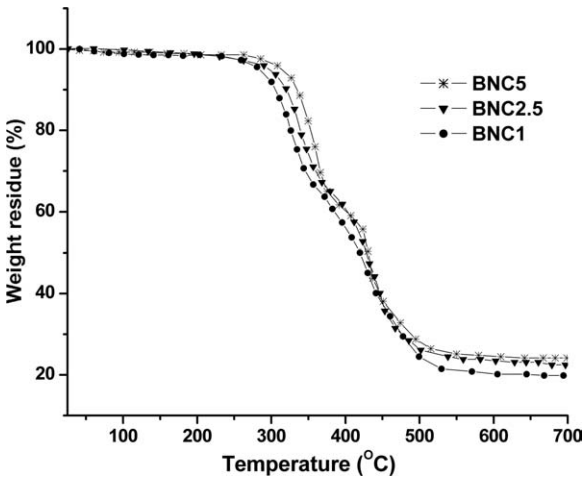

Figure 7 TGA thermograms for the nanocomposites.

of hydrogen bonding. Again, in the blend nanocomposites, the value was observed to increase with the OMMT loading from 0 to 5 wt %. This improvement was due to the imperative role of OMMT. The OMMT layers interacted with the polyester and the epoxy chains and restricted the mobility; this increased the strength of the nanocomposites films. Also, OMMT acted as a crack stopper with increasing OMMT content and formed a tortuous pathway for crack propagation; this resulted in an improved impact energy.[34]

The chemical resistances of the cured polyester/epoxy blends and nanocomposites were tested in various chemical environments (Table III) for 15 days at room temperature. All of the blends besides PEB3 and PEB4 showed relatively good alkali resistances because of the presence of a higher number of alkali-resistant ether and amide linkages in the system. The resistivity toward all of the media of all of the blends was also found to increase with the amount of epoxy resin. In the blend nanocomposites, with increasing clay loading, an improvement in the chemical resistance toward all of the media was observed. This was due to the interaction of the clay layers with the polyester chains, which resulted in the compact and crosslinked structure of the nanocomposites. The permeability of the nanocomposites was also reduced by the delamination of the clay layers through the insertion of the polymer chains; this, thereby, produced a tortuous pathway for diffusion. Because of this, the different ions or species present in the different media could not easily penetrate the surface, and the chemical resistance, thereby, increased.

Thermal properties

The thermogravimetric traces obtained for the polyester/epoxy blends and nanocomposites are shown in Figures 6 and 7. As shown in Figure 6,

the polyester/epoxy blends degraded by a two-step pattern. In the first step of degradation, the values of the onset thermal degradation temperature (T_{on}) and the ending thermal degradation temperature (T_{end}) for PEB1, PEB2, PEB3, and PEB4 were 273, 264, 256, and 242 and 378, 373, 362, and 349°C, respectively. However, in the second degradation step, the values were 410, 403, 400, and 393°C and 501, 496, 477, and 469°C, respectively. Thus, we observed that with increasing epoxy content, the thermal degradation temperature of the blends also increased. The weight residues also increased with increasing epoxy content and were 20, 19, 17, and 18% at 700°C for the blends PEB1, PEB2, PEB3, and PEB4, respectively. This higher thermostability of the blends was due to the better crosslinked structure formed by crosslinking between the free hydroxyl groups present in the fatty acids of the oil (present originally or generated during the amine crosslinking reaction) and the better physical interactions through hydrogen bonding, polar–polar interactions, and so on. Thus, because of the good compatibility between the alkyd and epoxy resins, the thermostability of the blends improved to a significant extent.

After the formation of the nanocomposites, the thermal degradation temperature of the blends improved further from 273 to 318°C with 0–5 wt % OMMT loadings. As shown in Figure 6, the first-step T_{on} and T_{end} values of BNC1, BNC2.5, and BNC5 were 287, 300, and 318 and 386, 398, and 401°C, respectively. Similarly, in the second step of thermal degradation of the blend nanocomposites, the T_{on} and T_{end} values were 406, 416, and 425 and 500, 514, and 529°C, respectively. This improvement of the thermal properties was mainly due to the effect of OMMT. The added clay enhanced the performance by acting as a superior insulator and mass-transport barrier to the volatile products generated during decomposition. The OMMT platelets hindered the diffusion of volatiles and assisted in the formation of char after thermal decomposition.[35,36] The degradation of polymers started with the formation of free radicals at weak bonds and/or chain ends; this was followed by their transfer to adjacent chains via interchain interactions. The improved thermal stability could also be explained through the reduced mobility of the polyester chains in the nanocomposite. Because of the interaction of the OMMT with the matrix, the motion of polymer chains was hindered. Also, OMMT served as a nucleation site for the enhanced crystallization of the nanocomposites. Because of reduced chain mobility, the chain-transfer reaction was suppressed, and consequently, the degradation process was slowed, and decomposition took place at high temperature.[37]

CONCLUSIONS

The results from this study indicate that vegetable-oil-based highly branched polyester resins could be successfully blended with vegetable-oil-based epoxy resin to enhance the physical, thermal, and mechanical properties and chemical resistance and to reduce the curing time and so on. The study revealed the formation of novel nanoscale hybrid composites by the inclusion of OMMT into the blend of *M. ferrea* L. seed oil based highly branched polyester and epoxy resins. The studies also showed that the addition of OMMT enhanced the mechanical properties, such as the tensile strength, impact resistance, and hardness, and the thermostability of the pristine system. The blend components showed good compatibility and interactions with OMMT, and thus, the studied nanocomposites could be used as multipurpose advanced thin-film materials.

The authors thank the Department of Physics of Tezpur University and North-Eastern Hills University (Shillong, India) for their help with the XRD analyses and SEM and TEM analyses, respectively.

References

1. Miyagawa, H.; Mohanty, A. K.; Burgueno, R.; Drzal, L. T.; Misra, M. Ind Eng Chem Res 2006, 45, 1014.
2. Uyama, H.; Kuwabara, M.; Tsujimoto, T.; Nakano, M.; Usuki, A.; Kobayashi, S. Chem Mater 2003, 15, 2492.
3. Ogunniyi, D. S.; Odetoye, T. E. Bioresour Technol 2008, 99, 1300.
4. Malshe, V. C.; Sikchi, M. Basics of Paint Technology; University Institute of Chemical Technology: Mumbai, 2004.
5. Oldring, P. K. T. Resins for Surface Coatings; Wiley: New York, 2000.
6. Athawale, V. D.; Chamankar, A. V. Paint India 2003, 53, 41.
7. Athawale, V. D.; Chamankar, A. V.; Athawale, M. Paint India 2000, 50, 39.
8. Cesteros, L. C.; Isasi, J. R.; Katime, I. J Polym Sci Part B: Polym Phys 1994, 32, 223.
9. Begawy, E. I.; Huglin, M. B. Eur Polym J 1991, 27, 1023.
10. Kim, B. K.; Oh, Y. S.; Lee, Y. M.; Yoon, L. K.; Lee, S. Polymer 2000, 41, 385.
11. Viswanath, G. R.; Thangaraj, R.; Guhanathan, S. Int J Polym Anal Char 2009, 14, 493.
12. Ahmad, S.; Ashraf, S. M.; Kumar, G. S.; Hasnat, A.; Sharmin, E. Prog Org Coat 2006, 56, 207.
13. Park, S. J.; Jin, F. L.; Lee, J. R. Mater Sci Eng A 2004, 374,109.
14. Yu, L.; Petinakis, S.; Dean, K.; Bilyk, A.; Wu, D. Macromol Symp 2007, 249, 535.
15. Haq, M.; Burgueño, R.; Mohanty, A. K.; Misra, M. Compos Sci Technol 2008, 68, 3344.
16. Torre, L.; Chieruzzi, M.; Kenny, J. M. J Appl Polym Sci 2010, 115, 3659.
17. Dutta, S.; Karak, N. Prog Org Coat 2005, 53, 147.
18. Deka, H.; Karak, N. J Appl Polym Sci 2010, 116, 106.
19. Das, G.; Karak, N. Prog Org Coat 2009, 66, 59.
20. Konwar, U.; Karak, N. Polym Plast Technol Eng 2009, 48, 970.
21. Konwar, U.; Karak, N.; Mandal, M. Polym Degrad Stab 2009, 94, 2221.
22. Dutta, N.; Karak, N.; Dolui, S. K. Prog Org Coat 2004, 49, 146.

23. Das, G.; Karak, N. Prog Org Coat 2010, 69, 495.
24. Lu, J.; Hong, C. K.; Wool, R. P. J Polym Sci Part B: Polym Phys 2004, 42, 1441.
25. Ray, S. S.; Bousmina, M. Prog Mater Sci 2005, 50, 962.
26. Miyagawa, H.; Misra, M.; Drzal, L. T.; Mohanty, A. K. Polymer 2005, 46, 445.
27. Maiti, P.; Batt, C. A.; Giannelis, E. P. Biomacromolecules 2007, 8, 3393.
28. Prabu, A. A.; Alagar, M. Prog Org Coat 2003, 49, 236.
29. Dutta, N.; Karak, N.; Dolui, S. K. J Appl Polym Sci 2006, 100, 516.
30. Lee, S. R.; Park, H. M.; Lim, H.; Kang, T.; Li, X.; Cho, W. J.; Ha, C. S. Polymer 2002, 43, 2495.
31. Lewitus, D.; McCarthy, S.; Ophir, A.; Kenig, S. J Polym Environ 2006, 14, 171.
32. Zhao, C. X.; Zhang, W. D. Eur Polym J 2008, 44, 1988.
33. Sinha, S. K.; Song, T.; Wan, X.; Tong, Y. Wear 2009, 266, 814.
34. Jawahar, P.; Balasubramanian, M. J Nanomater 2006, 4, 1.
35. Leszczýnska, A.; Njuguna, J.; Pielichowski, K.; Banerjee, J. R. Thermochim Acta 2007, 453, 75.
36. Chung, C. M.; Cho, S. Y.; Kim, J. G.; Oh, S. Y. J Appl Polym Sci 2007, 106, 2442.
37. Ray, S. S.; Okamoto, M. Prog Polym Sci 2003, 28, 1539.